Continuously Adaptive PI Control of Wave Energy Converters under Irregular Sea-State Conditions

Hoai-Nam Nguyen, Paolino Tona

Continuously Adaptive PI Control of Wave Energy Converters under Irregular Sea-State Conditions

Hoai–Nam Nguyen and Paolino Tona
IFP Energies nouvelles
IFPEN-Lyon, Rond-point de l'échangeur de Solaize, BP 3, 69360 Solaize, France
E-mail: {name.surname}@ifpen.fr

***Abstract*—The main objective in hydrodynamic control of wave energy converters (WECs) is the maximisation, for a broad range of sea states, of the energy captured from the waves. Latching control, model predictive control and "PID" control are examples of implementable strategies surveyed in the literature. "PID" control, while suboptimal, has the merit of being simple, requiring only straightforward calculations and can be considered a standard solution for WECs with a four-quadrant power take-off system (PTO), in particular in its "PI" variant. Adaptive PI control has been already discussed in the literature, usually using a gain-scheduling approach, with optimal gains precomputed offline for a representative set of sea states and applied as a function of estimated sea state conditions. In most literature, only average online estimations of sea states have been proposed, with time windows of several minutes. Such intermittent (or switching) adaptive control laws are clearly suboptimal in terms of energy recovery, since the control gains are not continuously updated whereas the sea state is continuously time-varying. In this paper we present a continuously adaptive PI control strategy, which takes into account (non-ideal) PTO efficiency. The problem of optimising the gains of the PI controller is converted into a convex optimisation problem, thus guaranteeing that a unique and optimal solution can be found offline. The gains of the PI controller are continuously adapted online, on a wave-to-wave basis, based on a real-time estimate of the dominant wave frequency of the wave force, which is in turn estimated from (normally) available WEC measurements. Validation is performed on a case study based on a lab-scale point-absorber WEC. Simulation results show that the proposed adaptive control scheme can recover more energy than a fixed-gain PI controller even in a sea state with constant spectral characteristics. Furthermore, in a changing sea state, it outperforms switching gain-scheduled PI control where the gains are updated from time to time based on an evaluation of the current sea conditions. Though some preliminary wave basin tests have already given encouraging results, further experiments are needed to precisely quantify its energy harvesting potential. Moreover, further research is needed to include WEC motion or actuator constraints in the optimisation procedure.**

***Index Terms*—Wave Energy Converters, PI Control, Conversion Efficiency, Adaptive Control, Unscented Kalman Filter, Dominant Frequency Estimation, Wave Force Estimation**

I. Introduction

The main objective in hydrodynamic control of wave energy converters (WECs) is the maximisation, for a broad range of sea states, of the energy captured from the waves. In many WECs, active control can be performed acting on the force applied by the power take-off system (PTO) on the oscillating body responsible of primary energy conversion (f_u in Fig. 1 which provides a simplified representation of a heaving-buoy WEC).

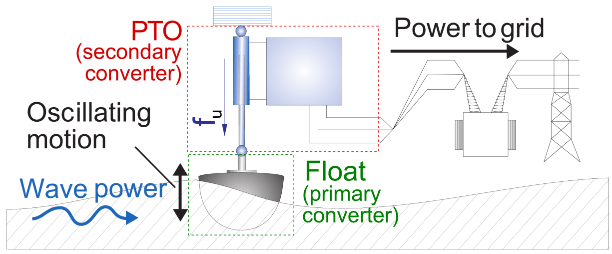

Fig. 1. Schematic diagram of a generic (heaving-buoy) wave energy converter

Among the implementable strategies surveyed in the literature, we can recall for instance, latching control, model predictive control and "PID" control [1]. While, in theory, latching control [2] and model predictive control [3], [4] allow to achieve high levels of energy capture, their practical implementation may be very challenging. This is due to the fact that these control strategies require a short-term prediction of wave excitation force, which can degrade the control performance, if the prediction is not perfect. Moreover, model predictive control, like other optimisation-based WEC control approaches, is a complex and computationally demanding algorithm.

"PID" control, on the other hand, has the merit of being simple, requiring only straightforward calculations [1]. Because of that, it was one of the first control strategy to be implemented on WEC prototypes (the "Salter's duck" [5], for instance). Even now, it can be considered a standard solution, when a four-quadrant PTO, capable of both harvesting and drawing power from the grid (respectively in generator and motor modes), is available. One embodiment of this approach is the PI (or BK) controller described in [6], which consists in computing the PTO force via a combined proportional feedback on the position and velocity of the oscillating element acting as primary converter (the float of Fig. 1)[1]. The damping controller (or P controller), where the PTO force is specified to be proportional to and oppositely directed to the velocity of the primary converter, is even more widely adopted, as it does not require the use of reactive power.

[1]This corresponds to a proportional–integral action on the velocity of the primary converter, which is the reason for it being (confusingly) referred to as a "PI" controller.

Assuming an ideal PTO (with 100 % conversion efficiency), well-established theoretical results are available to tune these kind of controllers for optimal energy recovery under the action of regular waves [7]. For practical applications, a dominant-frequency approximation is often used to extend these results to irregular sea-state conditions.

Whatever method is used to compute the P and I gains, they should not be kept constant, as the sea conditions change. Adaptive P or PI control has been already discussed in the literature [8]–[10], at different level of details, in the form of a gain-scheduling approach. The main idea is to compute optimal gains for a representative set of sea states. The gains are calculated offline, analytically or numerically, using a gridding approach: for each sea state, the ones leading to the best average power are picked. Then the appropriate control action f_u is found from a look-up table whose input is the current sea state, which can be identified, for instance, in terms of dominant wave period and significant wave height, or other characteristics of its spectrum. In most literature, only average online estimations of sea states have been proposed, with time windows of several minutes (10 minutes in [9], 20-30 minutes in [10]). Such intermittent (or switching) adaptive control laws are clearly suboptimal in terms of energy recovery, since the control gains are not continuously updated whereas the sea state is continuously time-varying.

In this paper we present a (truly) adaptive PI control strategy, which takes into account (non-ideal) PTO efficiency. The problem of optimising the gains of the PI controller is converted into a convex optimisation problem, thus guaranteeing that a unique and optimal solution can be found offline. The gains of the PI controller are continuously adapted online, on a wave-to-wave basis, based on a real-time estimate of the dominant wave frequency of the wave force, which is in turn estimated from (normally) available WEC measurements.

Section II describes the modelling assumptions and defines the control problem, along with the energetic performance criterion to be optimised. Section III presents the procedure to design an optimal PI control under regular waves in the presence of a non-ideal PTO. Section IV explains how the results from the previous section can be used, following a dominant wave frequency approach to deal with realistic polychromatic sea states, to build an adaptive control scheme: notably, the variable-gains PI control law requires a real-time estimate of the dominant frequency of the wave excitation force acting on the WEC, which has to be estimated as well since it is not normally available while the WEC is running. Section V introduces a case study, based on a lab-scale point-absorber WEC, and provides a preliminary assessment, in simulation, of the proposed control strategy. Finally, some concluding remarks end the paper.

II. WEC MODELLING AND CONTROL PROBLEM DEFINITION

A. WEC modelling

We consider here the type of WECs schematically represented in Fig. 1, that is, point-absorber WECs with an oscillating part that moves in one degree of freedom, the heaving direction for instance, with respect to a reference (fixed anchor or a submerged body). From the relative motion, useful energy can be extracted via the PTO.

Under the assumption that the oscillations of the system are relatively small, the WEC motion can be expressed, in the frequency domain, as follows [7],

$$\left(j\omega M + Z_{pa}(j\omega) + \frac{K_{pa}}{j\omega}\right) v(j\omega) = f_{ex}(j\omega) - f_u(j\omega) \quad (1)$$

where

- $v(j\omega)$ is the heaving velocity of the oscillating part;
- $f_{ex}(j\omega)$ and $f_u(j\omega)$ are the wave excitation force and the PTO force, respectively;
- M is the mass of the float with its connected parts;
- $Z_{pa}(j\omega)$ is the radiation impedance;
- K_{pa} is the stiffness coefficient.

Equation (1) is based on the Cummins integro-differential equation [11], whose hydrodynamic coefficients can be computed via boundary element method (BEM) software, such as WAMIT, Diodore, AQWA ou NEMOH. The radiation impedance $Z_{pa}(j\omega)$ is the result of an approximation of the radiation impulse response by an infinite impulse response filter and can be decomposed as

$$\begin{aligned} Z_{pa}(j\omega) &= B_{pa}(\omega) + j\omega(M_{pa}(\omega) + M_\infty) \\ &= H_{pa}(j\omega) + j\omega M_\infty \end{aligned} \quad (2)$$

where $B_{pa}(\omega)$ is the radiation resistance, and $M_{pa}(\omega)$ is the added mass after M_∞, the asymptotic value of the added mass for $\omega \to \infty$ is removed, $H_{pa} = B_{pa}(\omega) + j\omega M_{pa}(\omega)$. As in most modeling studies on point absorbers, it is assumed that viscous, frictional forces are negligible compared to the other terms in the equation of motion.

From (1), the float velocity can be rewritten as

$$v(j\omega) = \frac{1}{Z_i(j\omega)}(f_{ex}(j\omega) - f_u(j\omega)) \quad (3)$$

where the intrinsic impedance $Z_i(j\omega)$ is defined as

$$\begin{aligned} Z_i(j\omega) &= B_{pa}(\omega) + j\omega\left(M + M_\infty + M_{pa}(\omega) - \tfrac{K_{pa}}{\omega^2}\right) \\ &= R_i(\omega) + jX_i(\omega) \end{aligned} \quad (4)$$

where

$$\begin{cases} R_i(\omega) = B_{pa}(\omega), \\ X_i(\omega) = \omega\left(M + M_\infty + M_{pa}(\omega) - \tfrac{K_{pa}}{\omega^2}\right) \end{cases} \quad (5)$$

are, respectively, the intrinsic resistance and reactance.

B. Control structure

We define the control problem to be solved in the classic framework of impedance matching control for WECs [7].

In a monochromatic sea state, the wave excitation force is given as

$$f_{ex}(t) = Asin(\omega t + \phi) \quad (6)$$

where the phase ϕ can be set to be zero without loss of generality. Assuming that the control force is a linear feedback of the heaving velocity, see Fig. 2, its expression in the Laplace domain is

$$f_u(s) = Z_c(s)v(s) \tag{7}$$

where s is a complex number, $s = \sigma + j\omega$. Z_c can be seen as a load impedance, and designed following impedance-matching principles.

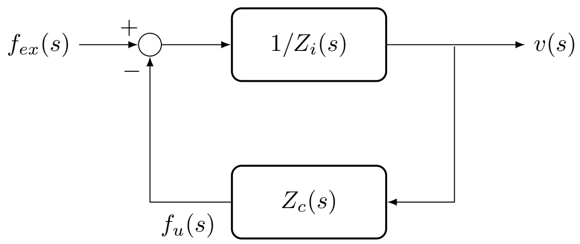

Fig. 2. Block diagram with WEC internal impedance $Z_i(s)$ and control impedance $Z_c(s)$.

The following proportional-integral (PI) control structure is chosen for the control block Z_c

$$f_u(t) = K_p v(t) + K_i \int_0^t v(\tau)d\tau \tag{8}$$

Rewriting (8) in the frequency domain

$$f_u(j\omega) = \left(K_p - j\frac{K_i}{\omega}\right) v(j\omega) \tag{9}$$

one obtains

$$\begin{cases} K_p = R_c, \\ K_i = -\omega X_c \end{cases} \tag{10}$$

where R_c and X_c are, respectively, the control (or load) resistance and reactance, i.e. $Z_c(j\omega) = R_c(\omega) + j\omega X_c(\omega)$.

C. Control objective

The control objective is to maximise the average (electric) power produced by the WEC

$$P_a = \frac{1}{T}\int_{t=0}^{T} \eta f_u(t)v(t)dt, \tag{11}$$

where η is the efficiency coefficient.

In the literature, it is generally assumed that $\eta = 1$, i.e. the PTO system is perfect [12], [13]. With this assumption, the mathematical procedure needed to calculate the optimal control action $f_u^*(t)$ is greatly simplified. For the case of regular waves, there exists an elegant analytical expression for $f_u^*(t)$ as a function of wave frequency. One of the well known results is that, in order to harvest the maximum amount of energy [14], the optimal velocity $v^*(t)$ should be in phase with the wave excitation force $f_{ex}(t)$. This result, however, does not hold if $\eta \neq 1$, as it will be shown later.

Unfortunately, the assumption of a perfect PTO with no conversion losses is unrealistic. The power that is withdrawn from the grid is always more expensive than the power that is delivered to the grid via the PTO. To take into account this fact, we can consider the efficiency coefficient η as a function of the ideal instantaneous power $f_u v$,

$$\eta(f_u v) = \begin{cases} \eta_p & \text{if} \quad f_u v \geq 0, \\ \eta_n & \text{if} \quad f_u v < 0 \end{cases} \tag{12}$$

where the coefficients $0 < \eta_p \leq 1$ and $\eta_n > 1$ depend on the PTO system, and may even be a function of $f_u v$.

III. Optimal PI control with non-ideal PTO under regular waves

A. Average power calculation

For the given wave excitation force (6) and the control force (7), it can be proved that the average power (11) is obtained as

$$P_a = \frac{A^2 R_c}{2\left((X_c + X_i)^2 + (R_c + R_i)^2\right)} C_\eta \tag{13}$$

where

$$C_\eta = \left(n_p - \frac{\eta_n - \eta_p}{\pi}\left(\frac{X_c}{R_c} - \arctan\left(\frac{X_c}{R_c}\right)\right)\right) \tag{14}$$

The proof is not detailed here for the sake of conciseness.

Indeed, if we consider the limit case when the PTO is perfect, i.e. $\eta_p = \eta_n = 1$, then $C_\eta = 1$ in (7) and the average power is calculated as

$$P_a = \frac{A^2 R_c}{2\left((X_c + X_i)^2 + (R_c + R_i)^2\right)} \tag{15}$$

which is the well-known result [14], obtained when the non-linear efficiency coefficient is not taken into account.

B. Optimal frequency response

Using (13), the next step is to compute the optimal R_c and X_c which maximise P_a. We require that $R_c \geq 0$, since R_c is used to convert the wave energy into useful mechanical or electrical energy. Notice that, because the factor $\frac{A^2}{2}$ has no influence on the optimal solution, it can be omitted in the optimisation problem. Thus, the problem to be solved is

$$\min_{R_c, X_c} \left\{ -\frac{R_c}{(X_c + X_i)^2 + (R_c + R_i)^2} C_\eta \right\} \tag{16}$$

With C_η defined by (14), (16) is clearly a nonlinear optimisation problem. Hence it is impossible to obtain a closed analytical form for the optimal solution.

Before proceeding further, define

$$d = \frac{X_c}{R_c}$$

Consider the function $f(p) = \eta_p - \frac{\eta_n - \eta_p}{\pi}(d - \arctan(d))$. By calculating the derivative of $f(p)$, it is easy to see that this function is monotonically non-increasing. Hence the equation,

$$\eta_p - \frac{\eta_n - \eta_p}{\pi}(d - \arctan(d)) = 0 \tag{17}$$

has a unique solution d^* for any positive η_n and η_p. Therefore, there exists a unique line

$$X_c = d^* R_c \tag{18}$$

that satisfies the equation

$$\eta_p - \frac{\eta_n - \eta_p}{\pi}\left(\frac{X_c}{R_c} - \arctan(\frac{X_c}{R_c})\right) = 0 \tag{19}$$

Figure 3 presents a numerical example of the average power P_a as a function of R_c, X_c for a given and fixed ω, using the WEC intrinsic impedance and the efficiency coefficients defined in the case study of Section V. Figure 4 shows a contour plot of P_a in the $R_c - X_c$ plane.

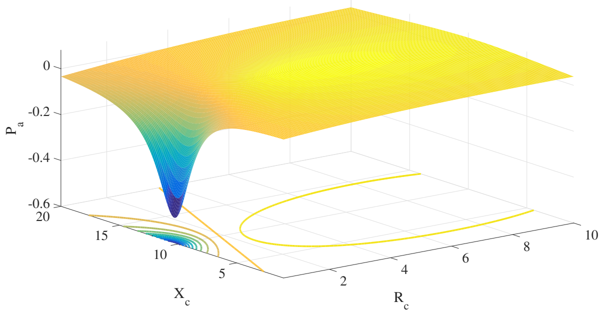

Fig. 3. Average power P_a as a function of R_c and X_c.

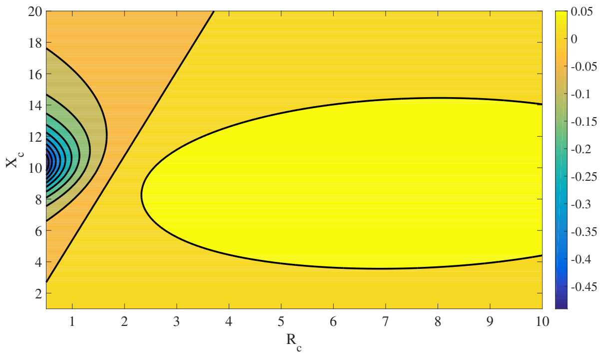

Fig. 4. Contour plot P_a in the $R_c - X_c$ plane.

Using Figures 3 and 4, two main remarks can be made

1) P_a is not a concave function of R_c and X_c.
2) The line (18) divides the plane $R_c - X_c$ into two regions
   - For all R_c, X_c such that
     $$X_c \geq d^* R_c$$
     the function P_a is convex.
   - For all R_c, X_c such that
     $$X_c \leq d^* R_c$$
     the function P_a is concave.

Figure 5 shows the average power P_a as a function of R_c and X_c in the concave region.

Figure 6 and Figure 7 show respectively, the optimal R_c and X_c (solid blue lines) as a function of ω. By solving (17), one obtains $d^* = 5.4403$ for the given η_p, η_n. Figure 6 and Figure 7 also show R_i and $-X_i$ (dashed red lines) as a function of ω.

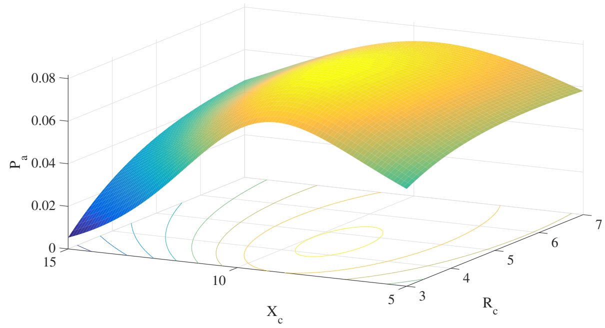

Fig. 5. Average power P_a as a function of R_c and X_c in a concave region.

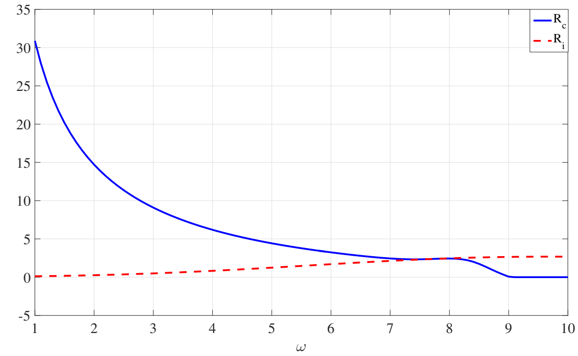

Fig. 6. Optimal R_c and R_i as a function of ω.

It can be noticed from Figure 7 that the optimal X_c is very close but not equal to $-X_i$. Hence the phase response $\angle W(s)$ of the transfer function (20) of the WEC system in closed loop

$$v(s) = \frac{1}{Z_i(s) + Z_c(s)} f_{ex}(s) = W(s) f_{ex}(s) \tag{20}$$

is in general not equal to zero. Hence the optimal velocity is in general not in phase with the wave excitation force in the presence of the nonlinear efficiency coefficient. The result of Falnes [14], where it is stated that the optimal velocity is in phase with the wave excitation force, can be considered only as an ideal case, where the PTO system is perfect.

Remark: If the PTO system is constrained to be purely resistive, then $X_c = 0$. In this case the optimisation problem

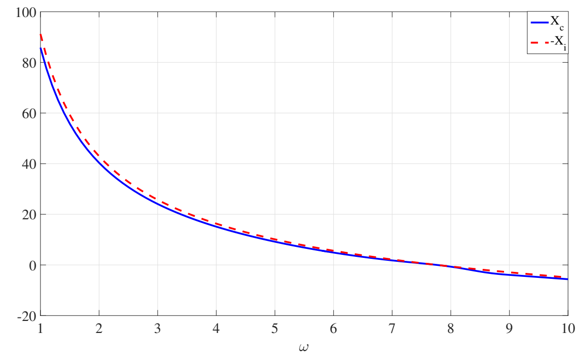

Fig. 7. Optimal X_c and $-X_i$ as a function of ω.

(16) becomes

$$\min_{R_c} \left\{ -\frac{n_p R_c}{X_i^2 + (R_c + R_i)^2} \right\} \quad (21)$$

There exists an analytical closed form solution to (21)

$$R_c = \sqrt{X_i^2 + R_i^2} \quad (22)$$

Note that the efficiency coefficient does not play any role in the optimal R_c in the resistive PTO system case. This is explained by the fact that there is no reactive power involved, so the energy harvested from the waves is always positive.

Figure 8 presents the optimal R_c as a function of frequency, for the purely resistive case.

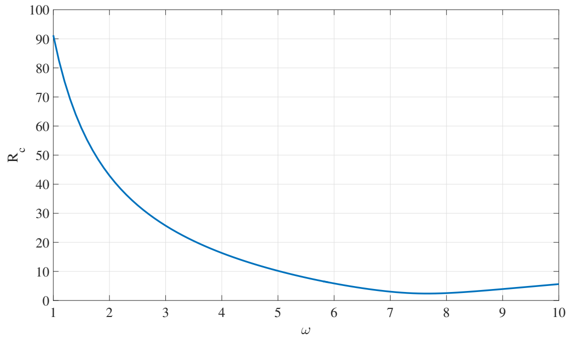

Fig. 8. Optimal R_c as a function of ω in the resistive PTO system case.

IV. Adaptive PI control

The approach described above allows to compute, for a specific WEC, the optimal control resistance R_c^o and reactance X_c^o, for each given regular wave excitation force.

Using (10), the corresponding optimal PI gains can be computed off-line, frequency by frequency, as:

$$\begin{cases} K_p^o = R_c^o(\omega), \\ K_i^o = -\omega X_c^o(\omega) \end{cases} \quad (23)$$

The resulting curves can be implemented, as look-up tables for instance, in an adaptive PI control scheme where the scheduling variable is the dominant frequency of the wave force excitation[2]. A customary approach in control of real devices is indeed to choose the load so that impedance matching occurs at the dominant frequency in a wave spectrum [15], though we should recall that the PI gains are truly optimal only in a harmonic excitation context. This approach is followed, for instance, for the design of the "simple-but-effective" controller in [16], a velocity tracking controller with adaptive parameters computed using online estimates of the dominant frequency and dominant amplitude of the wave excitation force.

The structure of the adaptive control scheme is shown in Fig. 9. Notice that the variable-gains PI control law requires an estimate of the dominant frequency of the wave excitation force as an input, and that the wave excitation force must be estimated as well, as it is a quantity that cannot be measured during normal WEC operation.

[2]The dominant frequency of the wave force is defined as the peak of its spectrum

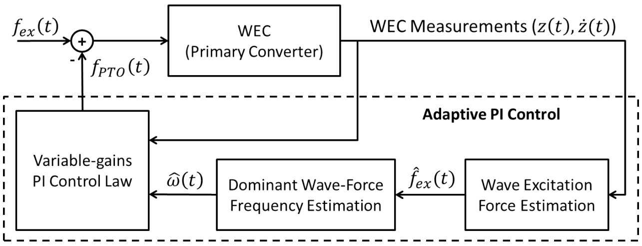

Fig. 9. Adaptive PI control approach.

To address the first problem, an estimation approach based on an extended Kalman filter (EKF), applied to a nonstationary, harmonic approximation of the wave excitation force, is proposed in [16]. However, it must be recalled that the EKF provides a solution to a nonlinear estimation problem via local linearisations of the underlying model. Thus, the variation of the wave force is large and/or the sampling time intervals are not sufficiently small, the linearisation may yield highly unstable filters, potentially leading to divergence phenomena [17], [18]. A more robust solution consists in estimating the dominant frequency (and amplitude) estimation using an unscented Kalman filter (UKF), as described in [19].

As to wave excitation force estimation, a few methods have been proposed recently and tested in real-time, in a model predictive control (MPC) framework (see for instance [20], [21], [22]), [23]). The method assessed in [23] (and fully described in [24]), based on a linear Kalman filter and a random walk model for the variation of the wave excitation force, has the main advantages of using only standard measurements for reactive control (position, velocity, PTO force) and of yielding quite accurate estimates over a large range of sea states.

V. Case study

In this section, we consider a lab-scale 1-DoF WEC system (described in [25]), whose intrinsic impedance can be modelled as the transfer function

$$Z_i(s) = \frac{s^6 + a_5 s^5 + a_4 s^4 + a_3 s^3 + a_2 s^2 + a_1 s}{b_7 s^7 + b_6 s^6 + b_5 s^5 + b_4 s^4 + b_3 s^3 + b_2 s^2 + b_1 s + b_0} \quad (24)$$

whose coefficients are given in TABLE I

Numerator	Denominator
	$b_7 = 1.44$
	$b_6 = 300.4$
$a_5 = 208.6$	$b_5 = 1.237 \times 10^5$
$a_4 = 8.583 \times 10^4$	$b_4 = 1.284 \times 10^7$
$a_3 = 8.899 \times 10^6$	$b_3 = 1.652 \times 10^8$
$a_2 = 1.074 \times 10^8$	$b_2 = 2.106 \times 10^9$
$a_1 = 7.031 \times 10^8$	$b_1 = 9.988 \times 10^9$
	$b_0 = 6.539 \times 10^{10}$

TABLE I
Model coefficients

Figure 10 presents the corresponding Bode plot, typical of WECs of the point-absorber type, with a resonance frequency of $f_r = 7.84$ rad/s.

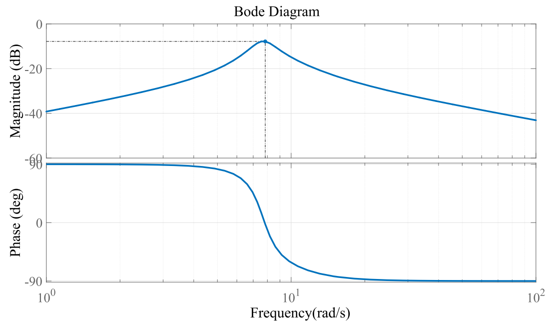

Fig. 10. Bode plot of the considered WEC system

PTO efficiency coefficients are $\eta_p = 0.8$, $\eta_n = 1.43$.

The idea is to compare the energy recovery performance of the proposed adaptive PI control using as a benchmark the (switching) gain-scheduled PI controller described in [26] and [27]. Thus, optimal K_p and K_i gains are computed offline over a set of sea states using a gridding approach: for each given sea state and considered time interval, the nominal WEC model is simulated in closed loops for a grid of gains, and the combination leading to the best average power P_a is picked. The control action is then to be determined from a look-up table with the current sea state (in terms of dominant wave period and significant height), being re-estimated at regular intervals, as an input. Notice, however, that the gain-scheduling mechanism has not been detailed in [26] nor in [27]: it has not been specified, for instance, if the gains are to be interpolated or chosen instead with a nearest-neighbour approach.

The same set of irregular waves, generated using a JONSWAP spectrum, which has been used to compute the optimal gains of the reference controller, is also used for validation. Of course, for a given irregular wave, the parameters of the switching gain-scheduled controller will not vary during the test, so the comparison is actually done with a fixed-parameters PI. The spectrum of the wave excitation force corresponding to one these irregular waves is shown in Fig. 11. Its dominant frequency is about 5 rad/s.

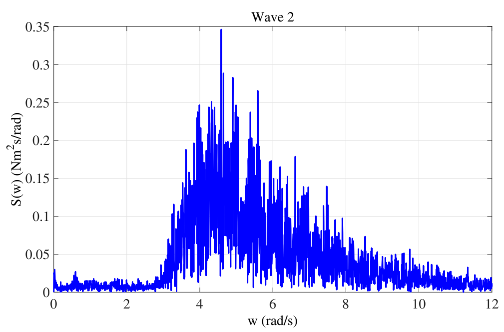

Fig. 11. First wave force spectrum (dominant frequency of ∼5 rad/s)

Fig. 12 shows respectively, the control input of the adaptive PI control (solid blue) and of the reference PI control (dashed red) over a 8-seconds long time interval. Fig. 13 shows the velocity of the adaptive PI control (solid blue), of the PI control (dashed red) and of the wave excitation force (dash-dot green), over the same time interval.

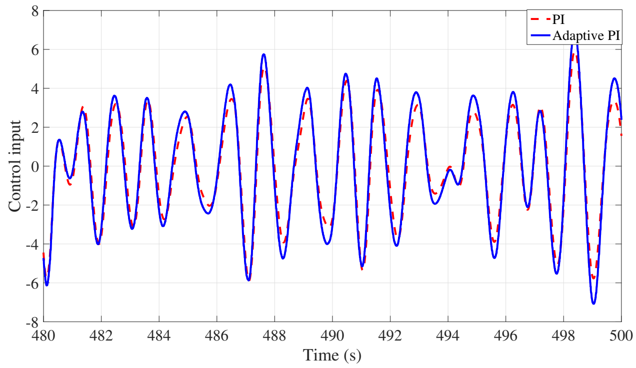

Fig. 12. Control input of the adaptive PI control law (solid blue), and of the PI control (dashed red) for the WEC system [26].

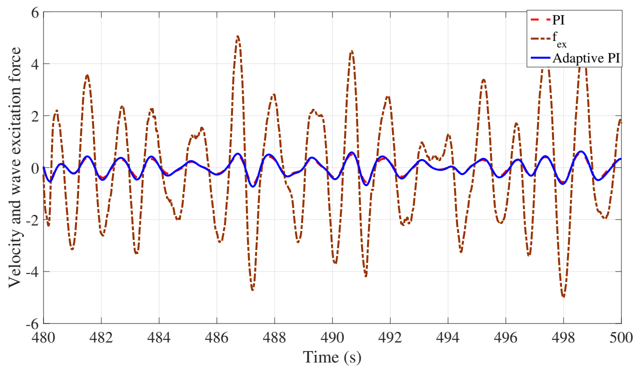

Fig. 13. Velocity of the adaptive PI control law (solid blue), and of the PI control (dashed red), and the wave excitation force (dash-dot brown) for the WEC system [26].

Finally, Fig. 14 presents the instantaneous power P_a for the adaptive PI control (solid blue) and for the PI control (dashed red). Fig. 15 shows the total accumulated energy for the adaptive PI control (solid blue) and for the reference PI control (dashed red). Interestingly, even in a test where the sea state is considered constant, the proposed adaptive PI control performs better than the reference PI control.

This is due to the continuous adaptation of PI gains to the dominant frequency estimate. Fig. 16 shows the variation of the dominant frequency estimate, obtained using the UKF approach mentioned in the previous section, over the last part of the test. Fig. 17 shows that the corresponding dominant magnitude estimated by the UKF (not used in the adaptive PI control law) follows well the wave force amplitude.

In order to validate the proposed adaptive control against a continuous change in sea state, corresponding to a transition from the wave of Fig. 11 to another wave, whose excitation

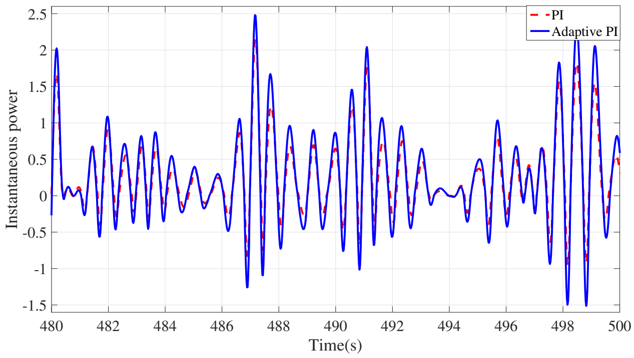

Fig. 14. Instantaneous power P_a of the adaptive PI control law (solid blue), and of the PI control (dashed red) for the WEC system.

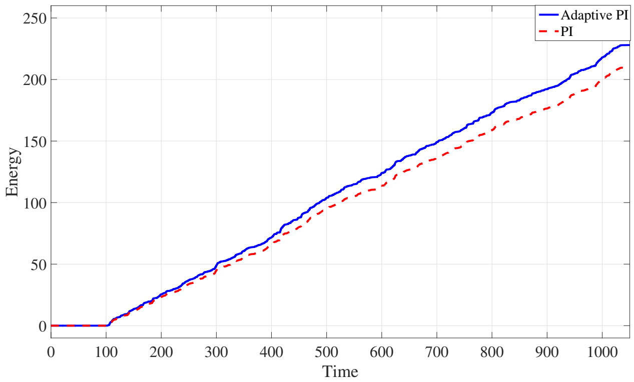

Fig. 15. Cumulative energy of the adaptive PI control law (solid blue), and of the PI control (dashed red) for the WEC system.

force is shown in Fig. 18, a second test is performed, under the excitation given by a wave force generated with a time-varying dominant frequency, which varies linearly from 5 rad/s to 2 rad/s.

For comparison purposes, a switching PI controller is implemented, using a table of optimal pre-computed gains for the two waves and for a set of intermediate sea states. The switching is performed on the basis of an average estimation of the dominant wave frequency. The first gain switch takes

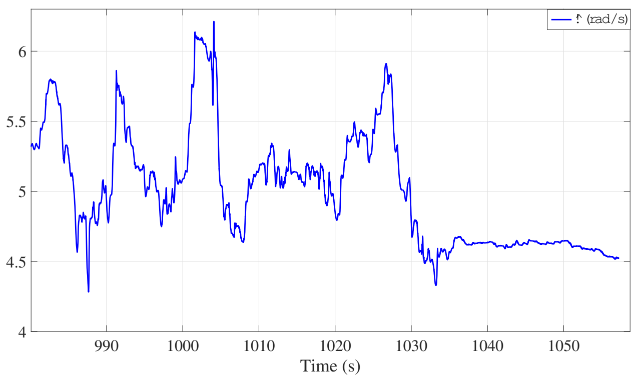

Fig. 16. Dominant wave force frequency estimation.

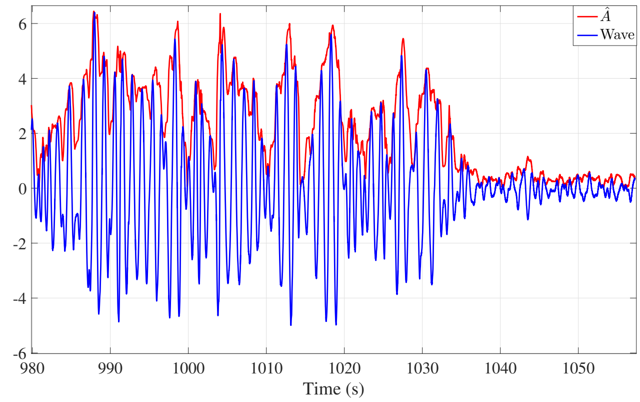

Fig. 17. Dominant wave magnitude estimation.

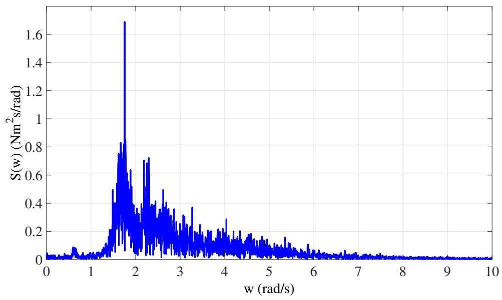

Fig. 18. Second wave force spectrum (dominant frequency of ∼2 rad/s)

place at $t = 200$ (which would correspond at about 15 minutes at full scale).

Fig.19 compares the energy harvesting performance of three controllers: adaptive PI, switching PI, and fixed-gains PI with gains optimised for the wave force of Fig. 11.

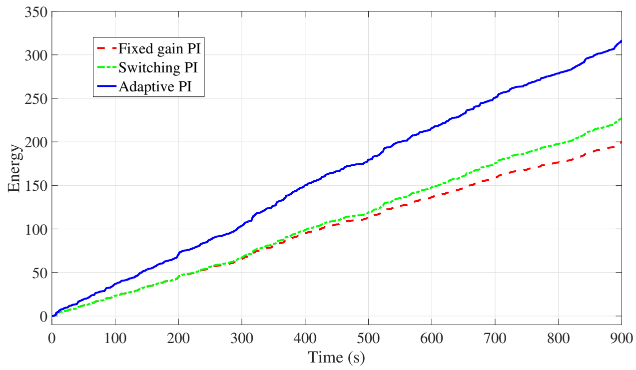

Fig. 19. Cumulative energy of the adaptive PI control law (solid blue), of the switching PI controller (dotted green) and of a fixed-gains PI controller with gains optimised for the first wave (dashed red).

VI. Conclusions

This paper focuses on a novel approach to design a continuously adaptive PI control strategy for wave energy converters.

A procedure, based on the solution of a convex optimisation problem, is presented, which allows to compute the optimal

PI gains for a given regular wave excitation force, while taking into account (non-ideal) PTO efficiency. It is shown that the optimal velocity is in general not in phase with the wave excitation force when realistic PTO efficiencies are considered. Optimal gain curves, as a function of frequency, can be obtained from this procedure, and implemented in an adaptive control scheme based on a dominant frequency approach. Combining two robust and accurate methods for real-time estimation of the wave excitation force from normally available WEC measurements and of the dominant frequency of the (estimated) wave excitation force, the gains of the PI controller can be continuously adapted online, on a wave-to-wave basis.

A case study, based on a lab-scale point-absorber WEC, has been used for validation. Simulation results show that the proposed adaptive control scheme can recover more energy than a fixed-gain PI controller even in a sea state with constant spectral characteristics. Furthermore, in a changing sea state, it outperforms switching gain-scheduled PI control where the gains are updated from time to time based on an evaluation of the current sea conditions.

In the future, a more extensive assessment is planned, both in simulation and through experimentation. Though the proposed adaptive PI control system has already been tested in a wave basin on the lab-scale prototype used as a case study, with encouraging results, further experiments are needed to precisely quantify its energy harvesting potential.

Finally, further research is needed to take into account WEC motion or actuator constraints (PTO force limits, stroke limits), which are not dealt with in the current optimisation procedure, as well as more complex WEC dynamics.

References

[1] J. Ringwood, "Control Optimisation and Parametric Design," in *Numerical Modelling of Wave Energy Converters*, M. Folley, Ed. Academic Press, 2016, pp. 229 – 251.

[2] F. Saupe, Y. Creff, J.-C. Gilloteaux, P. Bozonnet, and P. Tona, "Latching control strategies for a heaving buoy wave energy generator in a random sea," in *IFAC World Congress*, vol. 19, no. 1, 2014, pp. 7710–7716.

[3] J. Cretel, A. Lewis, G. Lightbody, and G. Thomas, "An application of model predictive control to a wave energy point absorber," in *Control Methodologies and Technology for Energy Efficiency*, vol. 1, no. 1, 2010, pp. 267–272.

[4] J. Hals, J. Falnes, and M. Torgeir, "Constrained optimal control of a heaving buoy wave-energy converter," *J. Offshore Mech. Arct. Eng.*, vol. 133 (1), 2010.

[5] S. Salter, "Development of the duck concept," in *Wave Energy Conference*, Heathrow, U.K., 1978.

[6] E. V. Sanchez, R. H. Hansen, and M. M. Kramer, "Control performance assessment and design of optimal control to harvest ocean energy," *Oceanic Engineering, IEEE Journal of*, vol. 40, no. 1, pp. 15–26, Jan 2015.

[7] J. Falnes, *Ocean waves and oscillating systems: linear interactions including wave-energy extraction*. Cambridge University Press, 2002.

[8] T. Whittaker, D. Collier, M. Folley, M. Osterried, A. Henry, and M. Crowley, "The development of oystera shallow water surging wave energy converter," in *Proceedings of the 7th European Wave and Tidal Energy Conference, Porto, Portugal*, 2007, pp. 11–14.

[9] R. H. Hansen and M. M. Kramer, "Modelling and control of the wavestar prototype," in *Proceedings of 2011 European Wave and Tidal Energy Conference*, 2011.

[10] J. Hals, J. Falnes, and T. Moan, "A comparison of selected strategies for adaptive control of wave energy converters," *Journal of Offshore Mechanics and Arctic Engineering*, vol. 133, no. 3, p. 031101, 2011.

[11] W. Cummins, "The impulse response function and ship motions," DTIC Document, Tech. Rep., 1962.

[12] J. Falnes, "A review of wave-energy extraction," *Marine Structures*, vol. 20, no. 4, pp. 185–201, 2007.

[13] J. Hals, J. Falnes, and T. Moan, "Constrained optimal control of a heaving buoy wave-energy converter," *Journal of Offshore Mechanics and Arctic Engineering*, vol. 133, no. 1, p. 011401, 2011.

[14] J. Falnes, *Ocean waves and oscillating systems: linear interactions including wave-energy extraction*. Cambridge university press, 2002.

[15] U. Korde and J. Ringwood, *Hydrodynamic Control of Wave Energy Devices*. Cambridge University Press, 2016.

[16] F. Fusco and J. V. Ringwood, "A simple and effective real-time controller for wave energy converters," *Sustainable Energy, IEEE Transactions on*, vol. 4, no. 1, pp. 21–30, 2013.

[17] S. J. Julier, J. K. Uhlmann, and H. F. Durrant-Whyte, "A new approach for filtering nonlinear systems," in *American Control Conference, Proceedings of the 1995*, vol. 3. IEEE, 1995, pp. 1628–1632.

[18] S. J. Julier and J. K. Uhlmann, "New extension of the kalman filter to nonlinear systems," in *AeroSense'97*. International Society for Optics and Photonics, 1997, pp. 182–193.

[19] H. Nguyen, P. Tona, and G. Sabiron, "Dominant wave frequency and amplitude estimation for adaptive control of wave energy converters," in *MTS/IEEE OCEANS 2017 Conference*, Aberdeen, U.K., 1978.

[20] P. Kracht, S. Perez-Becker, J.-B. Richard, and B. Fischer, "Performance improvement of a point absorber wave energy converter by application of an observer-based control: Results from wave tank testing," *IEEE Transactions on Industry Applications*, vol. 51, no. 4, pp. 3426–3434, 2015.

[21] B. A. Ling, "Real-time estimation and prediction of wave excitation forces for wave energy control applications," Ph.D. dissertation, Oregon State University, 2015.

[22] O. Abdelkhalik, S. Zou, R. Robinett, G. Bacelli, and D. Wilson, "Estimation of excitation forces for wave energy converters control using pressure measurements," *International Journal of Control*, pp. 1–13, 2016.

[23] H.-N. Nguyen, G. Sabiron, P. Tona, M. Kramer, and E. Vidal-Sanchez, "Experimental validation of a nonlinear MPC strategy for a wave energy converter prototype," in *ASME International Conference on Offshore Mechanics and Arctic Engineering*, 2016.

[24] H.-N. Nguyen and P. Tona, "Wave excitation force estimation for wave energy converters of the point absorber type," *IEEE Transactions on Control System Technology*, 2017, (submitted for publication).

[25] M. Møller Jakobsen, F. Ferri, and M. Kramer, "Practical performance of control strategies for point absorbers," in *Proceedings of the 11th European Wave and Tidal Energy Conference*, 2015.

[26] R. H. Hansen, M. M. Kramer, and E. Vidal, "Discrete displacement hydraulic power take-off system for the wavestar wave energy converter," *Energies*, vol. 6, no. 8, pp. 4001–4044, 2013.

[27] E. V. Sánchez, R. H. Hansen, and M. M. Kramer, "Control performance assessment and design of optimal control to harvest ocean energy," *IEEE Journal of Oceanic Engineering*, vol. 40, no. 1, pp. 15–26, 2015.